

Bogoliubov excitation spectrum in anharmonic traps

E Gershnabel, N Katz, E Rowen,* and N Davidson
*Department of Physics of Complex Systems,
Weizmann Institute of Science, Rehovot 76100, Israel*

We study the linearized Bogoliubov excitation spectrum of infinitely long anharmonically trapped Bose-Einstein condensates, with the aim of overcoming inhomogeneous broadening. We compare the Bogoliubov spectrum of a harmonic trap with that of a theoretical flat-bottom trap and find a dramatic reduction in the inhomogeneous broadening of the lineshape of Bogoliubov excitations. While the Bragg excitation spectrum for a condensate in a harmonic trap supports a number of radial modes, the flat trap is found to significantly support just one mode. We also study the excitation spectrum of realistic anharmonic traps with potentials of finite power dependence on the radial coordinate. We observe a correlation between the number of radial modes and the number of bound states in the effective potential of the quasi-particles. Finally we compare a full numerical Gross-Pitaevskii simulation of a finite-length condensate to our model of infinite, linearized Gross-Pitaevskii excitations. We conclude that our model captures the essential physics.

I. INTRODUCTION

The spectrum of weak excitations over the ground state of a Bose-Einstein condensate (BEC) has been found to obey the Bogoliubov dispersion relation [1]. There is however, a finite width to the dynamical structure factor $S(k, \omega)$ which characterizes the response of the BEC to an exciting field with momentum k and frequency ω . Usually the exciting field is in a Bragg configuration [2], where k is the momentum difference of two laser beams, and ω is the detuning between the two. There is a small intrinsic width originating from the Beliaev decay of quasi-particles which is usually dominated by broadening due to finite time of the Bragg pulse and inhomogeneity of the condensate. The latter heavily depends upon the trap geometry. In some cases the wavelength of an excitation is much shorter than the condensate dimensions. Under these circumstances it is justified to employ the local density approximation (LDA) [3]. For cigar shaped condensates, the radial dimension is sometimes comparable to the excitation wavelength, leading to the breakdown of the LDA, and the appearance of radial modes [4, 5]. Avoiding inhomogeneous broadening is possible in the spectral domain using echo spectroscopy where a degenerate Bragg pulse transfers Bogoliubov excitations with wavenumber $+k$ to $-k$ [6], and in the time domain where rapid oscillations cause a suppression of inhomogeneous mean field and of Doppler dephasing [7]. Suppression of the inhomogeneity mechanisms, allows longer coherence times, and opens the possibility of studying the homogeneous broadening mechanisms, that reflect the intrinsic decoherence processes of the bulk excitations, e.g. elastic collisions with the BEC [8].

In this paper we propose the use of a flat-bottom trap in order to reduce the inhomogeneous broadening of Bogoliubov excitations in a BEC. We restrict ourselves to the cigar shaped geometry, in which the inhomogeneity is mainly manifested by the presence of many radial modes. By linearizing the Gross-Pitaevskii equation (GPE), assuming a uniform and infinite potential in the axial direction and using a quasiparticle projection method [5], we obtain the Bogoliubov excitation spectrum for a flat-bottom trap. Then, we compare the above results to the excitation spectrum of a harmonically trapped BEC. A clear reduction in the inhomogeneous broadening is evident by comparing between the two spectra. This result, although intuitive, is not trivial for two reasons. The first is that even in a flat trap the density is not constant, but varies over a distance characterized by the healing length ξ .

The second reason is that even a hypothetical homogeneous finite condensate supports several radial modes. Indeed, we find that it is the gradual decay of the density to zero at the trap boundary that reduces the coupling to the high order radial modes. The envelope of both harmonic and flat trap spectra are found to match the LDA [3]. We then examine the excitation spectrum of a condensate trapped in the power-law potential $V = \kappa_\rho \rho^p$, where ρ is the radial coordinate, and p is an even integer. We observe the substantial excitation of a second radial mode in the spectrum, and demonstrate its suppression using higher order potentials. The transition between potentials supporting one or two radial modes is explained by an effective potential picture. Finally, we solve the full GPE and find the Bogoliubov spectrum for a realistic, experimentally feasible [9] three-dimensional axially elongated trap, confined both in the radial and axial direction using a high-order potential. The spectrum obtained by the linearized approach where the

*Electronic address: eitan.rowen@weizmann.ac.il

potential is axially uniform, and by the full GPE for an elongated condensate, are found to be qualitatively similar due to the tight radial confinement.

The outline of the paper is as follows: in section II, we study the ground state and the quasiparticles of the flat-bottom trap, then in section III, a comparison between the flat-bottom trap and the harmonic trap excitation spectra is given. In section IV we study high order anharmonic potentials, still axially infinite, and section V is devoted to the full GPE calculation of a three dimensional elongated anharmonic trap.

II. GROUND STATE AND BOGOLIUBOV QUASI-PARTICLES IN AN INFINITE CYLINDER

Since the traps discussed in this paper are cigar shaped, the dominant contribution to the inhomogeneity originates from the trap geometry in the radial direction. Thus we first assume an infinite trap in the axial direction \hat{z} . We solve the linearized GPE for a flat-bottom trap, uniform in the axial direction. In order to compare with our harmonic trap, we fix the chemical potential $\mu/\hbar = 2.06$ kHz (in the Thomas-Fermi approximation) and the number of atoms per unit length $N = 10^5$ atoms per $L = 52.2\mu\text{m}$ to coincide with our BEC experimental parameters [1].

Our flat-bottom trap potential, is a cylindrically symmetric hard-wall confinement in the radial direction:

$$V_T(\mathbf{r}) = \begin{cases} 0 & \rho < R_{TF} \\ \infty & \text{otherwise} \end{cases} \quad (1)$$

where R_{TF} is the radial Thomas-Fermi radius, which is determined by the constraints on μ and N/L . We calculate the Bogoliubov spectrum for the flat-bottom trap following the derivation of [5] for harmonic traps. Briefly, in the linear regime, the condensate wavefunction can be expanded as:

$$\Psi(\mathbf{r}, t) = e^{i(\mu/\hbar)t} \{ \psi_0(\mathbf{r}) + \sum_j [c_j u_j(\mathbf{r}) e^{-i\omega_j t} + c_j^* v_j^*(\mathbf{r}) e^{i\omega_j t}] \} \quad (2)$$

where the c_j 's are constants, and u and v are the quasi-particle amplitudes, that obey the following orthogonality and symmetry relations:

$$\int d\mathbf{r} \{ u_i u_j^* - v_i v_j^* \} = \delta_{ij}; \quad \int d\mathbf{r} \{ u_i v_j - v_i u_j \} = 0 \quad (3)$$

The wavefunction expansion in equation 2 is inserted into the GPE: $i\hbar \frac{\partial}{\partial t} \Psi = \left(-\frac{\hbar^2 \nabla^2}{2m} + V_T + g|\Psi|^2 \right) \Psi$, where $g = \frac{4\pi\hbar^2 a}{m}$ is the coupling constant, m is the atomic mass and a is the s -wave scattering length. For a cylindrical condensate, infinite in the axial direction, we define $\psi_0(\rho, z) = \phi_0(\rho)/L$, $(u, v)_{n,k}(\rho, z) = \frac{1}{\sqrt{L}} e^{ikz} (u, v)_{n,k}(\rho)$ as the new ground state wavefunction and the quasi-particle amplitudes, respectively. Gathering terms to zero order u, v yields the stationary GPE:

$$\left(-\frac{\hbar^2 \nabla_\rho^2}{2m} + V_T(\rho) + \frac{gN}{L} \phi_0(\rho)^2 \right) \phi_0(\rho) = \mu \phi_0(\rho) \quad (4)$$

The next order gives the coupled equations:

$$\hbar\omega_{n,k} u_{n,k}(\rho) = \left[-\frac{\hbar^2 \nabla_\rho^2}{2m} + \frac{\hbar^2 k^2}{2m} + V_T(\rho) - \mu + \frac{2gN}{L} \phi_0^2(\rho) \right] u_{n,k}(\rho) + \frac{gN}{L} \phi_0^2(\rho) v_{n,k}(\rho) \quad (5)$$

$$-\hbar\omega_{n,k} v_{n,k}(\rho) = \left[-\frac{\hbar^2 \nabla_\rho^2}{2m} + \frac{\hbar^2 k^2}{2m} + V_T(\rho) - \mu + \frac{2gN}{L} \phi_0^2(\rho) \right] v_{n,k}(\rho) + \frac{gN}{L} \phi_0^2(\rho) u_{n,k}(\rho) \quad (6)$$

also known as the linearized GPE or Bogoliubov equations.

First, we find the ground state wavefunction from equation 4 by applying imaginary time evolution [10] to the Thomas-Fermi wavefunction [11]. Figure 1 shows the ground state wavefunctions for the flat-bottom trap (solid line) and for an axially infinite harmonic trap (dashed line), with a confining potential of $V_T = \frac{1}{2} m \omega_\rho^2 \rho^2$ where $\omega_\rho = 2\pi \times 226\text{Hz}$ [6]. Indeed, the harmonic trap wavefunction is similar to the Thomas Fermi ansatz, and the flat trap has a ground state in which the density drops to zero at R_{TF} over a length scale $\xi = (8\pi n(0)a)^{-1/2}$ [11], where $n(0)$ is the peak density.

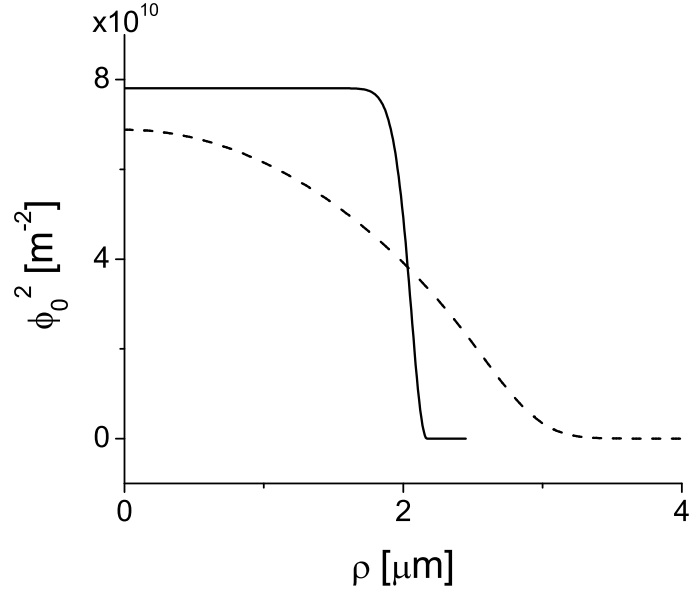


FIG. 1: Ground state radial wavefunctions of axially infinite harmonic (dashed line) and flat-bottom (solid line) traps obtained by solving the stationary GPE with imaginary time evolution.

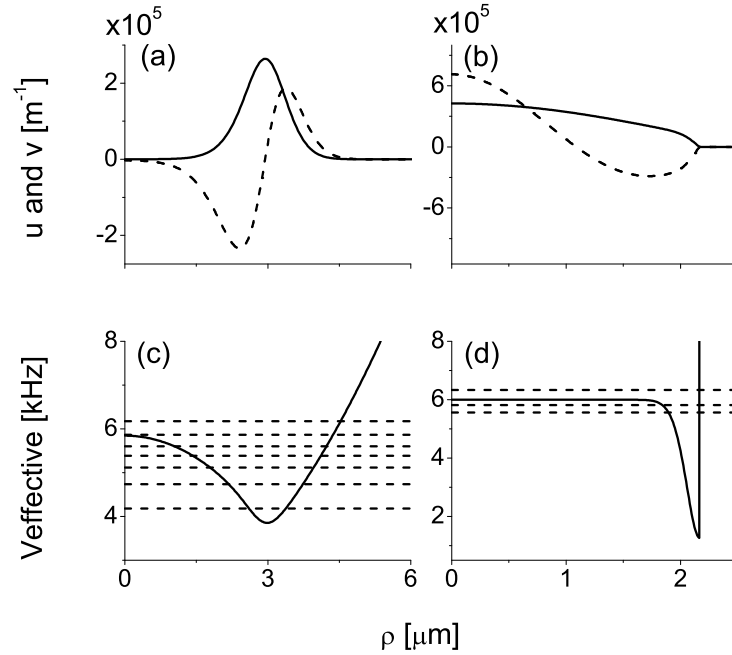


FIG. 2: Quasi-particles amplitudes $u_{n,k}$ and effective potentials. (a) Harmonic trap, $u_{0,k}$ (solid line) and $u_{1,k}$ (dashed line). (b) Flat-bottom trap, $u_{0,k}$ (solid line) and $u_{1,k}$ (dashed line). (c) Harmonic trap, effective potential (solid line) and Bogoliubov frequencies (dashed line). (d) Flat-bottom trap, effective potential (solid line) and Bogoliubov frequencies (dashed line).

In order to find the Bogoliubov frequencies $w_{n,k}$ and the quasi-particles amplitudes $(u, v)_{n,k}$, the relaxed wavefunction is substituted in equations 5 and 6. The Bogoliubov equations 5 and 6 are an eigenvalue problem and are solved by expanding the functions $u(\rho)$ and $v(\rho)$ using a complete set of zero order Bessel functions. The problem is thus reduced to a matrix diagonalization and is numerically solved [5]. We take the excitation momentum k to be $k = 8.06 \mu\text{m}^{-1}$ as in [6].

The calculated lowest order quasi-particle amplitudes $u_{0,k}$ (zero order, solid lines) and $u_{1,k}$ (first order, dashed

lines) are shown in figure 2(a) and (b), for the harmonic and flat-bottom trap, respectively. For the n^{th} order radial modes, both u and v have n nodes.

Comparing figures 2(a) and (b) reveals a dramatic difference. For the flat bottom trap (figure 2(b)) $u_{0,k}$ and $u_{1,k}$ are mainly centered around $\rho = 0$ whereas for the harmonic trap (figure 2(a)) they are significantly shifted.

To qualitatively explain this effect we approximate equation 5 as:

$$\hbar\omega_{n,k}u_{n,k}(\rho) = [-\frac{\hbar^2\nabla_\rho^2}{2m} + \frac{\hbar^2k^2}{2m} + V_T(\rho) - \mu + \frac{2gN}{L}\phi_0^2(\rho)]u_{n,k}(\rho) \quad (7)$$

where we neglect the contribution of v , which are small for the $k\xi > 1$ regime considered here. The two Bogoliubov equations 5 and 6 are thus reduced to a Schrödinger equation for the excitations, with the effective potential $V_{eff} = \frac{\hbar^2k^2}{2m} + V_T(\rho) - \mu + \frac{2gN}{L}\phi_0^2(\rho)$ [12]. In figure 2(c) and (d) we plot the effective potential for the harmonic and flat-bottom trap, respectively. The dashed lines are the lowest eigenvalues $\omega_{n,k}$ of equations 5 and 6, without neglecting v . The effective potential of the harmonic trap can be approximated for the lowest modes as a harmonic potential, leading to $u(\rho)_{n,k}$ which resemble eigenstates of the harmonic trap for ω_n sufficiently deep in the effective trap. However, for eigen-energies $\hbar\omega_{n,k}$ which approach the effective trap height, there is a nonvanishing amplitude that interferes constructively near $\rho = 0$ due to radial symmetry, so that the amplitude is not concentrated in the well. This happens even for the lowest mode in the flat trap. The well in this case is extremely narrow, originating only from the spatially smoothing of the ϕ_0 at the walls, supporting no “bound states” concentrated in the well.

III. BOGOLIUBOV BRAGG SPECTROSCOPY OF A FLAT-BOTTOM TRAP

Once the quasi-particles amplitudes and the Bogoliubov frequencies are obtained, they can be used to derive the Bogoliubov Bragg spectrum, using the quasi-particle projection method [5]. Briefly, in this method the c_j coefficients in equation 2 are taken to be time-dependent and then substituted into the GPE, which includes now also the Bragg external potential $V_B \cos(kz - \omega t)$, where V_B is the strength of the Bragg potential. The momentum given to the condensate, in the Bragg process, defined as:

$$P_z(t) = \frac{\hbar}{2i} \int d\mathbf{r} \Psi^*(\mathbf{r}, t) \frac{\partial}{\partial z} \Psi(\mathbf{r}, t) + c.c. \quad (8)$$

is found to be [5]:

$$P_z(t) = \frac{NqV_B^2t^2}{4\hbar} \sum_n |W_{n,k}|^2 \left[\left(\frac{\sin[(\omega_{n,k} - \omega)t/2]}{(\omega_{n,k} - \omega)t/2} \right)^2 - \left(\frac{\sin[(\omega_{n,k} + \omega)t/2]}{(\omega_{n,k} + \omega)t/2} \right)^2 \right] \quad (9)$$

where $W_{n,k} = 2\pi \int d\rho \rho [u_{n,k}^*(\rho) + v_{n,k}^*(\rho)]\phi_0(\rho)$. $W_{n,k}$ can be considered as a weight function that determines the weight of each radial mode. This weight is given by the overlap between the ground state and the quasi-particles amplitudes $(u, v)_{n,k}$.

Figure 3a and 3b show the linearized spectrum (solid lines) obtained from equation 9 for the $k = 8.06\mu m^{-1}$ momentum, after application of a 4.2 ms Bragg pulse, in the harmonic and flat-bottom trap, respectively. The harmonic trap spectrum of figure 3(a) shows four resolved radial modes. It is similar to the Bragg spectrum obtained from full GPE calculation, for harmonically trapped elongated BEC (figure 2a in [6]), as also noted in [5]. The lowest radial mode has a small overlap with the ground state, due to its ring shape, as seen in figure 2(a). This ring shape can be explained using energy considerations. Due to exchange symmetry, the mean-field energy of an excitation is twice that of the ground state, making it more favorable to concentrate the quasiparticle in a ring around the ground-state. In the effective potential picture, the minimum of the well is near the Thomas-Fermi radius for exactly this reason. The spectrum may thus be qualitatively described by the following argument. For the lowest radial mode, the overlap of the excitation wavefunction, which is approximately gaussian, with the condensate wavefunction is small. As the radial number n increases, but remains small enough for the effective potential to be approximated by a harmonic oscillator the overlap with the ground state increases since the quasiparticle wavefunction is wider. Upon further increasing n , the oscillations in u and v wash out any overlap with the condensate.

From figure 3(b) it is apparent that the flat-bottom trap supports mainly the first radial mode, strongly suppressing the excitation of higher order modes, even though they are valid solutions to the Bogoliubov equations. This suppression is due to the small overlap $W_{n,k}$ between the quasiparticle amplitude for $n > 0$ and the ground state, as seen from figures 1 (solid line) and 2(b). There are no states deep in the well of the effective potential, and since only $u_{0,k}$ is nodeless it has the dominant overlap with ϕ_0 . In the Thomas-Fermi limit of an effective potential of a

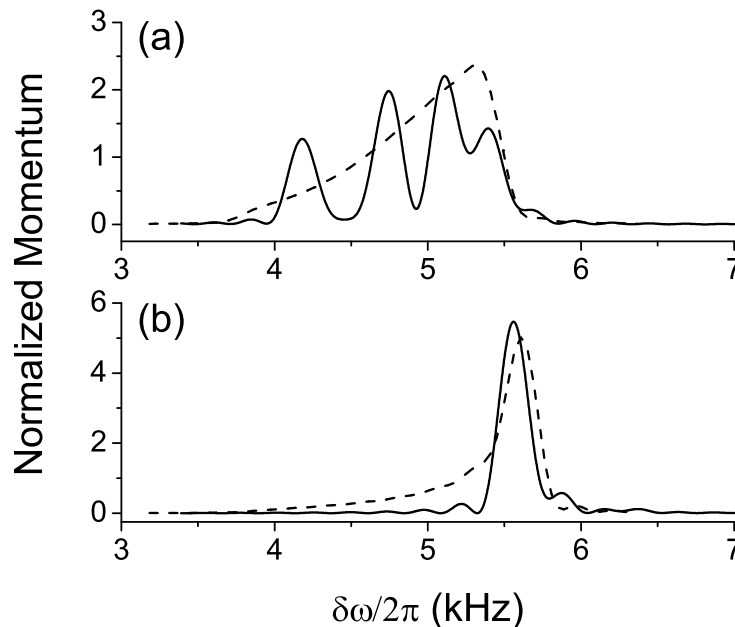


FIG. 3: Bragg spectra for Bogoliubov (extremely weak Bragg pulses) excitations. (a) Harmonic trap. (b) Flat-bottom trap. Solid line corresponds with the linearized GPE solution, dashed line corresponds with the LDA. The y axis is the quantity $P_z/(NV_B^2\hbar k)$ in units of $(\hbar\omega_\rho)^{-2}$.

cylindrical well with infinite walls, the quasi-particle states are Bessel functions of order 0, J_0 . This approximation yields a significant overlap between u and ϕ_0 for a number of radial modes. The overlap decays as $1/n$ for large n . Only when considering the relaxed wavefunction, which is closer in shape to the function J_0 , does the lowest radial mode become dominant.

It is insightful to compare these results to the inhomogeneous line shape calculated within the LDA [3], shown as dashed lines in figure 3. The LDA lineshapes were obtained by integration over the structure factor weighted by the inhomogeneous density distribution of the relaxed wavefunctions. The simplified LDA picture, whose basic assumptions are invalid here indeed fails to produce the radial mode structure. Surprisingly, it is seen from figure 3 that it describes the envelope of the spectrum for both traps quite well, suppressing modes outside it [5].

IV. OTHER CYLINDRICAL ANHARMONIC TRAPS

So far, an idealized infinite cylindrical trap was studied. However, such a trap cannot be realized and therefore we consider experimentally achievable traps of finite high-order potentials [9]. Here we show that even rather steep potential may yield deviations from the single-mode spectrum of the flat-bottom trap. This is done by evaluation of the Bogoliubov excitation spectrum for $k = 8.06\mu m^{-1}$, in axially infinite traps with anharmonic radial potentials of the form $V_T(\mathbf{r}) = \kappa_\rho \rho^p$ with $2 \leq p \leq 20$, using the procedure described above to solve the linearized GPE. The number of atoms per unit length is chosen to be the same as in section II. The chemical potential is the same for all traps, but different than that in section II.

The resulting spectra for the potential of ρ^{10} and ρ^{20} are shown in figures 4(a) and (b). A strong suppression of modes is apparent, in comparison to the number of modes in the harmonic trap (figure 3(a)). The appearance of a second radial mode in the ρ^{10} and not in the ρ^{20} trap seems surprising considering the flatness of both potentials. The qualitative difference between the two traps, which leads to such different response can be seen in the effective potentials plotted in figure 5. In the effective potential picture of the ρ^{10} trap (figure 5(a)) we discern two trapped energy states, whereas for the ρ^{20} trap (figure 5(b)) we observe only one “bound” eigen-state, while the higher modes are now “free”. This leads to a dramatic change in the Bragg coupling matrix elements, suppressing all higher order radial modes, although these modes are within the allowed LDA envelope. Note that this picture is only approximate due to the neglect of the v terms. Interesting corrections are expected at lower $k\xi$, where the v contribution is no longer negligible. Also, the effective Schrödinger equation is radial, leading to constructive interference near $\rho = 0$.

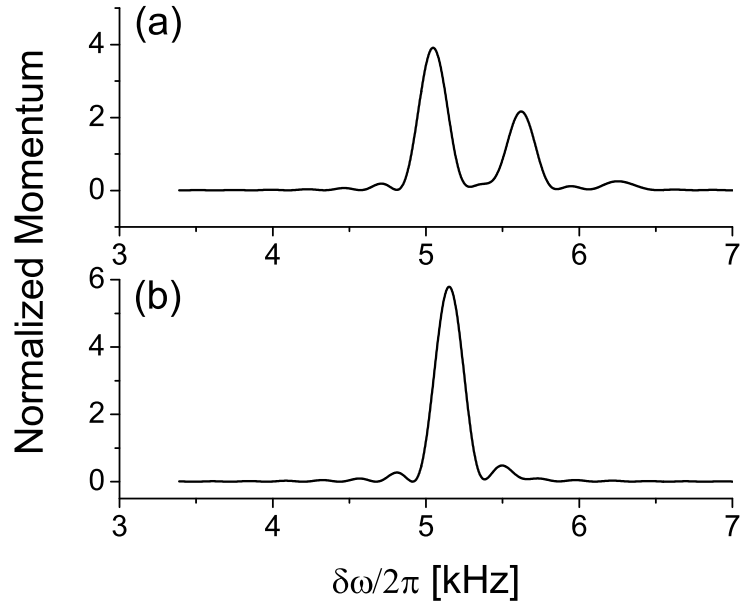


FIG. 4: Bragg spectra for Bogoliubov excitations. (a) ρ^{10} trap. (b) ρ^{20} trap. The y axis is the quantity $P_z/(NV_B^2\hbar k)$ in units of $(\hbar\omega_\rho)^{-2}$.

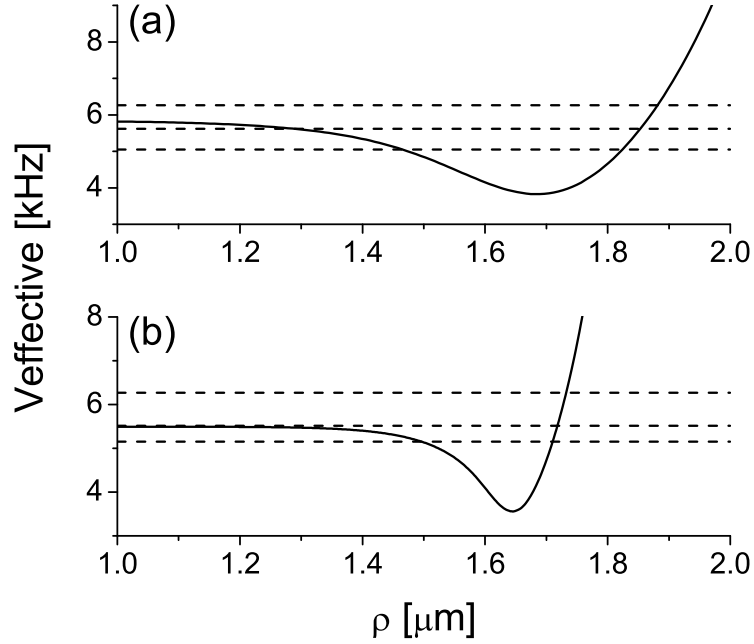


FIG. 5: Effective potentials (solid lines) and linearized GPE Bogoliubov frequencies (dashed lines) (a) ρ^{10} trap. (b) ρ^{20} trap.

We calculated the Bragg spectra for the Bogoliubov excitations for other values of p , and found a monotonic reduction in the weight of the higher order radial modes with increasing steepness of the radial potential.

V. REALISTIC THREE-DIMENSIONAL ANHARMONIC TRAPS

Finally, we compare between the spectra obtained above with the linearized GPE for cylindrical traps, with no axial confinement, and the spectra obtained for realistic elongated condensates confined in similar experimentally-realizable

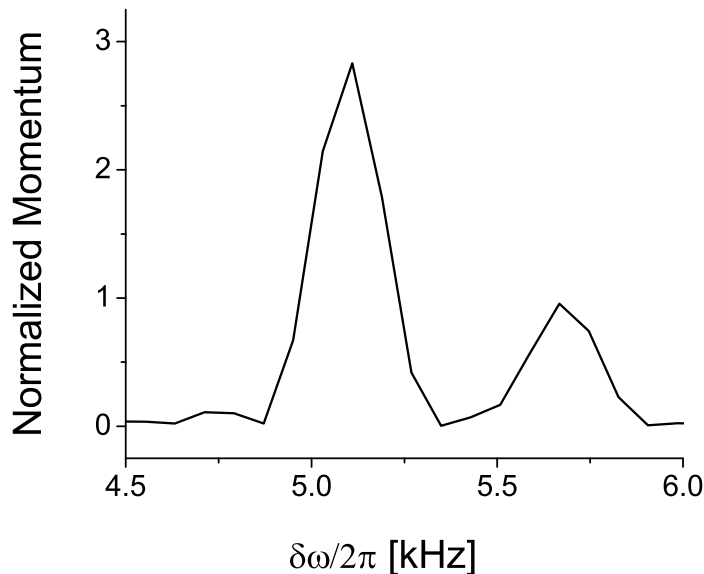


FIG. 6: Bogoliubov spectra for the potential $V_T(\mathbf{r}) = \kappa_\rho \rho^{20} + \kappa_z z^{12}$, using the full GPE.

three-dimensional anharmonic traps. We consider one specific optical trap generating a potential $V_T(\mathbf{r}) = \kappa_\rho \rho^{20} + \kappa_z z^{12}$ which is very similar to the one used experimentally for the atom-optics billiard of [13].

For this we numerically solve the full GPE $i\hbar\partial_t\psi = \{-\hbar^2\nabla^2/(2m) + V + g|\psi|^2\}\psi$, with $V(\mathbf{r}, t) = V_T(\mathbf{r}) + V_B \cos(kz - \omega t)$. We evolve ψ on a two dimensional grid (using the cylindrical symmetry of the problem) $N_z \times N_r = 2048 \times 32$, using the Crank-Nicholson differencing method. We ignore the influence of gravity to keep the cylindrical symmetry of the problem. Experimentally, gravitation may be compensated for using a magnetic field [14].

The Bogoliubov Bragg spectrum thus calculated is shown in figure 6. Comparison between figure 6 and figure 4b, indicates a qualitative similarity between the spectra of the “real” three-dimensional traps and that of their idealized axially infinite (two-dimensional) version, even though figure 6 includes additional inhomogeneity due to axial confinement, as well as possible finite-size (Doppler) effects [2, 7]. Thus we see the essence of the inhomogeneous broadening is indeed captured by the radial dependence of the trap.

VI. CONCLUSION

In conclusion, we propose and study a possible approach to reduce the inhomogeneity of trapped condensates by changing the functional form of the trap. We show a reduction of the inhomogeneous line-shape and suppression of the multiple peaked structure in the Bragg Bogoliubov spectra by using anharmonic traps with steep walls. The suppression is found to be monotonic with the steepness of trap potential walls. Linearized calculations for simplified two-dimensional cylindrical traps give qualitative understanding of the suppression of high-order radial modes, due to decreasing overlap with the ground-state wave function. Further LDA calculations we performed, suggest a dramatic broadening of the spectra in the presence of gravity, emphasizing the necessity to compensate for gravity in experimental realization of the anharmonic traps. Finally, full GPE simulation of the spectra with previously used optical traps confirm the experimental feasibility of this approach. The reduction in inhomogeneous broadening opens the possibility to study the more intrinsic homogenous broadening mechanisms. Experimental realization of BEC confined by anharmonic traps should also yield new experimental opportunities, such as the sharpening of the phase transition from superfluid to Mott-insulator [15] and rich variety of vortex phases [16].

This work was supported in part by the Israel Ministry of Science and the Israel Science Foundation. The authors wish to express their gratitude to C. Tozzo and F. Dalfovo for their assistance.

References

- [1] Steinhauer J, Ozeri R, Katz N and Davidson N 2002 *Phys. Rev. Lett.* **88** 120407
- [2] Stenger J, Inouye S, Chikkatur A P, Stamper-Kurn D M, Pritchard D E and Ketterle W 1999 *Phys. Rev. Lett.* **82** 4569,
Stenger J, Inouye S, Chikkatur A P, Stamper-Kurn D M, Pritchard D E and Ketterle W 2000 *Phys. Rev. Lett.* **84** 2283
- [3] Brunello A, Dalfovo F, Pitaevskii L, Stringari S and Zambelli F 2001 *Phys. Rev. A.* **64** 063614
- [4] Steinhauer J, Katz N, Ozeri R, Davidson N, Tozzo C and Dalfovo F 2003 *Phys. Rev. Lett.* **90** 060404
- [5] Tozzo C and Dalfovo F 2003 *New J. Phys.* **5** 54
- [6] Gershnabel E, Katz N, Ozeri R, Rowen E, Steinhauer J and Davidson N 2003 *Phys. Rev. A*, in press, cond-mat/0309584
- [7] Katz N, Ozeri R, Rowen E, Gershnabel E and Davidson N 2003 *Preprint*, cond-mat/0308492
- [8] Katz N, Steinhauer J, Ozeri R and Davidson N 2002 *Phys. Rev. Lett.* **89** 220401
- [9] Friedman N, Kaplan A and Davidson N 2002 *Adv. At. Mol. Opt. Phys.* **48** 99
- [10] Dalfovo F and Stringari S 1996 *Phys. Rev. A.* **53** 2477
- [11] Dalfovo F, Giorgini S, Pitaevskii L and Stringari S 1999 *Rev. Mod. Phys.* **71** 463
- [12] Pitaevskii L and Stringari S 2003 *Bose-Einstein Condensation*, (Oxford: Oxford University Press) p 211
- [13] Friedman N, Kaplan A, Carasso D and Davidson N 2001 *Phys. Rev. Lett.* **86** 1518
- [14] Monroe C, Swann W, Robinson H and Wieman C 1990 *Phys. Rev. Lett.* **65** 1571
- [15] Greiner M, Mandel O, Esslinger T, Hänsch T W and Bloch I 2002 *Nature* **415** 39
- [16] Baym G and Kavoulakis G M 2003 *New J. Phys.* **5** 51